ACTA MICROBIOLOGICA BULGARICA Volume 37 / 2 (2021)

# Mycosynthesis and Characterization of Gold and Silver Nanoparticles Using Biomolecules of *Pleurotus ostreatus* as Antibacterial Agent against Some Selected Pathogens

Bukola Christianah Adebayo-Tayo*, Joshua Olusegun Ogunrinade

*Department of Microbiology, University of Ibadan, Ibadan, Oyo State, Nigeria.*

**Abstract**

The study aims to investigate the biosynthesis and characterization of gold (AuNPs) and silver nanoparticles (SNPs) using biomolecules: exopolysaccharides (EPS), culture-free filtrate (CFF) and fruiting body extract (FBE) of *Pleurotus ostreatus* (PO), and to evaluate the antibacterial potential of the nanoparticles against some pathogens. The nanoparticles were characterized by UV-visible spectra, FTIR and SEM. Nanoparticles formation was confirmed by changes in colour; colour changes from pale yellow to purple, cloudy colourless to purple and yellow to dark purple indicate, respectively, POEPSAuNPs, POCFFAuNPs and POFBEAuNPs formation. Colour changes from pale yellow, cloudy colourless and yellow to dark brown indicate POEPSSNPs, POCFFSNPs and POFBESNPs formation, respectively. Surface plasmon resonance (SRP) peaks were observed at 400 nm. SEM revealed POEPSAuNPs, POCFFAuNPs and POCFFAuNPs as polymorphic with sizes ranging from 0.5 – 2.6 µm, 0.08 - 1.00 µm, and 0.2 – 2.4 µm. POEPSSNPs, POCFFSNPs and POFBESNPs were aggregate particles with sizes of 0.2 - 3.0 µm, 0.2 - 2.8 µm, and 0.1 – 3.2 µm. FTIR showed that amide, carboxyl and hydroxyl groups contributed to nanoparticles biosynthesis. The AuNPs exhibited a broad spectrum of activity against the tested pathogens compared to the SNPs. POEPSAuNPs and POFBEAuNPs had the highest inhibitory activity against *E. coli* while POFBEAuNPs had the highest inhibitory activity against *Micrococcus* sp. with MIC of 0.2 at 200 µg/mL, and POEPSSNPs and POCFFSNPs had the highest inhibitory activity against *S. aureus* with MIC of 0.05 at 50 µg/mL. In conclusion, biomolecules from *P. ostreatus* supported the biosynthesis of nanoparticles with enhanced therapeutic properties.

**Keywords:** *Pleurotus ostreatus,* exopolysaccharides, culture-free filtrate, gold and silver nanoparticles, antibacterial activity, pathogen.

**Резюме**

Целта на това проучване е да се изследва биосинтезата и охарактеризирането на златни (AuNPs) и сребърни наночастици (SNP) с помощта на биомолекули: екзополизахариди (EPS), отдекантирана културелна супернатанта (CFF) и екстракт от плодно тяло (FBE) на *Pleurotus ostreatus* (PO), както и да се направи оценка на антибактериалния потенциал на тези наночастици срещу някои патогени. Наночастиците са охарактеризирани с UV/Vis спектрофотометър, FTIR и SEM. Образуването на наночастици се потвърждава от промени в цвета от бледожълто до лилаво, от безцветно облачно до лилаво, както и от жълто до тъмно лилаво, което съответсва на образуването на POEPSAuNPs, POCFFAuNPs и POFBEAuNPs. Промените в цвета от бледожълто, безцветно облачно и жълто до тъмнокафяво показват съответно образуването на POEPSSNPs, POCFFSNPs и POFBESNPs. Наблюдавани се пикове на повърхностния плазмен резонанс (SRP) при 400 nm. Чрез SEM POEPSAuNPs, POCFFAuNPs и POCFFAuNPs се визуализират като полиморфни частици с размери, вариращи от 0.5 – 2.6 µm, от 0.08 – 1.00 µm и от 0.2 – 2.4 µm. POEPSSNPs, POCFFSNPs и POFBESNPs се виждат като агрегирани частици с размери от 0.2 – 3.0 µm, от 0.2 – 2.8 µm и от 0.1 – 3.2 µm. Чрез FTIR се доказва, че амидните, карбоксилните и хидроксилните групи участват в биосинтезата на наночастиците. AuNPs показва широк спектър на антибактериална активност срещу тестваните патогени в сравнение с SNPs. POEPSAuNPs и POFBEAuNPs имат най-висока инхибиторна активност срещу E. coli, докато POF-

* Corresponding author: bukola.tayo@gmail.com

BEAuNPs проявяват най-висока инхибиторна активност срещу *Micrococcus sp.* с MIC 0,2 при. 200 µg/ml, а POEPSSNPs и POCFFSNPs имат най-висока инхибиторна активност срещу *S. aureus* с MIC 0.05 при 50 µg/ml. В заключение, изследването демонстрира, че биомолекулите от *P. ostreatus* поддържат биосинтезата на наночастици с повишени терапевтични свойства.

**Introduction**

The increased resistance of pathogenic bacteria to conventional antibiotics has led to an inroad into a novel field called nanotechnology. This is a science that combines biology, chemistry, and physics for the synthesis of nano-scale particles that have numerous applications (Rezaei-Zarchi *et al*., 2012; Demir *et al*., 2014). The field of nano-science and technology have gained great importance because of its potential applications in various areas such as chemicals, textile industries, materials industry, medical diagnostic (future nanobots), drug and gene delivery and electronics, diagnosis, artificial implants, tissues engineering, computing, biochemical sensors, medical imaging and so on (Huang *et al*., 2003; Ghosh *et al.*, 2008; Pissuwan *et al.*, 2010; Pissuwan *et al*., 2011; Saha *et al*., 2012). Moreover, it provides a platform to modify and develop metals of unique properties to form nanoparticles having promising applications in diagnostics, biomarkers, cell labelling, contrast agents for biological imaging, antimicrobial agents, drug delivery systems and nano-drugs for treatment of various diseases (Coster *et al*., 2010). They have been used to produce nanoparticles and these are referred to as the building blocks of nanotechnology. Nanoparticles can be produced using physical, chemical and biological methods and the latter method is considered to be safe and eco-friendly.

Although biological methods involve the use of bacteria, fungi, yeast, actinomycetes and higher plants, fungi are considered a reliable source of metabolites that can be used to biosynthesize nanoparticles (Phanjom *et al*., 2015). Mushrooms, a higher fungus, are gourmet cuisine with a high nutritional value and therapeutic properties, and also known to contain metabolites that have been confirmed to have antimicrobial effect, a good example being *P. ostreatus*, a cosmopolitan mushroom. Metabolites such as polysaccharides and cell-free filtrates of mushrooms may act as both reducing and capping agents in nanoparticle biosynthesis, thus producing bio-compatible and bio-stable nano-sized particles. The use of mushrooms in nanotechnology derives from the large production of bioactive compounds that are eco-friendly bio-reductants, such as proteins, polysaccharides and enzymes (Castro-Longoria *et al*., 2011). These have been used for pharmaceutical purposes due to their diverse biological activities that include anti-tumour and immunomodulation activities. It is usually secreted into the environment and is known to reduce heavy metals in their surroundings because of the functional groups (hydroxyl groups) and metal salt precursors they possess (Mata *et al*., 2004). Since fungi are very effective secretors of extracellular compounds, therefore, achieving a vast production of bioactive compounds. Also, the economic viability and facility of employing biomass are another merit of the utilization of a green fungal-mediated approach to synthesize metallic nanoparticles. Moreover, a number of species grow fast and therefore culturing and keeping them in the laboratory are very simple (Castro-Longoria *et al*., 2011). In the present scenario, nanomaterials emerged as novel antimicrobial agents and this is due to their high surface area to volume, unique chemical and physical properties, and ability to concentrate conventional antibiotics when used in synergy (Kim *et al*., 2003).

The most studied aspect of nanotechnology is its ability to offer an opportunity to fight drug resistance. The mechanism of action of nanoparticles is quite different from that of antibiotics, thus nanoparticles are safe, economical and cost effective to combat the challenges in future (Fayaz *et al*., 2011).

Biologically inspired nanoparticles synthesis is currently a rapidly expanding area of research in nanotechnology owing to their many advantages, with silver nanoparticles (SNPs) and gold nanoparticle (AuNPs) being the most studied of the metals. Among nanoparticles, SNPs possess higher antibacterial activity against gram-negative and gram-positive microorganisms. Factors such as solvent choice, non-toxic stabilization material and environmental benign reducing agent are the factors that are responsible for the biosynthesis of biologically safe nanoparticles. Also, gold nanoparticles, apart from their antibiotic capabilities, have been used in nano-imaging due to their bio-compatibility, stability and bio-reduction ability. Gold nanoparticles in peptidoglycan will disturb the crystalline process of peptidoglycan by forming an amorphous region around them, which will reduce the capacity to resist pressure from the inside of cell walls. Usually, peptidoglycan has a crystalline structure that is resistant against the high osmotic pressure inside the cell, which may reach 20

atmospheres in the case of gram-positive bacteria. The nanoparticles will act as destruction triggering points of cell walls. In addition, gold nanoparticles can be utilized as energy sources of physical energy under the fields of electromagnetic waves, X-ray or ultrasound to damage cell walls or chromosomes, leading to the suppression of bacteria growth.

Silver nanoparticles (SNPs) attached to the surface of bacteria based on size. All SNPs were found to be highly toxic to the bacterial strains and their antibacterial efficacy increased by lowering particle size. This effect was significantly enhanced as the size of nanoparticles approached the sub-10nm range and5nm SNPs demonstrated the fastest bactericidal activity as compared to 7nm and 10nm SNPs at their respective, minimum bactericidal concentration. The bacterial membrane contains sulphur-containing proteins, and the silver nanoparticles interact with these proteins in the cell as well as with the phosphorus-containing compounds like DNA (Marini *et al*., 2007). Silver has a greater affinity to bind with the sulphur- and phosphorus-containing bio-molecules of the cell. Therefore, sulphur-containing proteins in the cell membrane, inside the cells and phosphorus-containing elements like DNA are likely to be the preferred sites for binding of silver nanoparticles. If silver nanoparticles enter the bacterial cell, they form a low molecular weight region in the centre of the bacteria to which the bacteria conglomerates, thus protecting the DNA from the silver ions. The nanoparticles preferably attack the respiratory chain, cell division finally leading to cell death. The nanoparticles release silver ions in the bacterial cells, which enhances their bactericidal activity (Rai *et al*., 2009).

Increasing resistance of pathogenic strains to antibiotics has led to failure in the treatment of infectious diseases and this is a major challenge in the medical and pharmaceutical fields. These major strains include *Escherichia coli, Staphylococcus aureus, Pseudomonas aeruginosa,* and *Klebsiella pneumonia* (Fayaz *et al*., 2011). Different infections by drug resistant strains have been reported worldwide and are considered major pathogen of community and hospital-acquired infections. These have resulted into high mortality and morbidity rate and the treatments are getting difficult as a result of high resistance to antibiotics. Drug resistance, especially in recent decades, has led to the search for different approaches and methods for finding new compounds against bacteria and fungi. Nanoparticles have dimensions of 100 nm or less. They have gained remarkable attention because of their unusual properties and the various applications they are suited for, when compared to their bulkier counterparts (Kato *et al*., 2011). These features have helped spread the use of nanomaterials at a faster rate day by day. They can be used to fight against germs, in diagnostics and treatment of diseases, water and air purification, food production, cosmetics, and clothing (Aitken *et al*., 2006). Silver is the most commonly used engineering nanomaterial in all consumer products (Akinoglu *et al*., 2014). Mycosynthesis and characterization of gold and silver nanoparticles using EPS and CFF and FBE of *P. ostreatus* and its antibacterial potential against some selected pathogens was investigated.

## Materials and Methods

*Sample collection and culture preparation*

*P. ostreatus* samples were purchased from FoodCo in Ibadan, Oyo state, Nigeria. Mycelium was obtained by tissue culturing, pure cultures were obtained by sub-culturing and the stock culture was maintained on PDA supplemented with 0.5% yeast extract stored at 4°C on PDA slants (Jonathan and Fasidi, 2003).

Clinical isolates of *K. pneumonia, Bacillus cereus, P. aeruginosa, Micrococcus* sp., *E. coli* and *S. aureus* were collected from the culture collection of the Environmental Unit of the Department of Microbiology and Department of Pharmacy, University of Ibadan.

Production of biomolecules (CFF, EPS and FBE) from P. ostreatus mycelium

*P. ostreatus* mycelium was cultured in Potato Dextrose Broth (PDB) for CFF production. The sterile PDB was inoculated with the mycelial culture and incubated at 28°C for 7 days. The fermentation broth was filtered to remove the mycelium. The mycelium was washed 3 - 4 times to remove any attached media component. Ten g of the mycelial biomass was suspended in 100 ml sterilized distilled water and kept for 3 days at 28°C under shaking conditions at 150 rpm. The biomass was filtered using Whatman No.1 filter paper to obtain CFF. The CFF was kept at 4°C for further use.

EPS production was done using Mushroom Complete Medium (MCM) containing glucose (20 g/L), peptone (3 g/L), yeast extract (5 g/L), $KHPO_4$(0.2), $K_2PO_4$ and $NH_3SO_4$ using the modified method of Cui *et al*. (2007) with some modifications. Sterile MCM was inoculated with young *P. ostreatus* culture (3-day-old) and incubated at 28°C for 20 days. The fermentation broth was filtered

and the EPS was precipitated using cold absolute ethanol at 4°C for 24 hrs. The precipitate EPS was obtained by centrifugation at 12,000 rpms for 15 mins. The total sugar concentration was determined by the phenol-sulphuric acid method using glucose as a standard (Dubois *et al*., 1956). The exopolysaccharide production was expressed as mg/L. The EPS was further dried at 60°C to remove the ethanol content.

*Production of fruiting body extracts from the fruiting body of P. ostreatus*

The fruiting body extract was obtained from the fruiting body of *P. ostratus* according to the method of Felek *et al*. (2015). 5 g of oven dried milled sample was soaked in sterile distilled water. The soaked sample was boiled for 30 mins and then allowed to cool. The cooled sample was incubated for 24 hrs at 35°C. The resulting leachate was filtered and labeled FBE and stored at 4□C for further use. The POEPS, POCFF and POFBE were used for nanoparticles biosynthesis.

*Biosynthesis of AuNPs and SNPs using POEPS*

AuNPs biosynthesis using POEPS was done by adding 30 mL of 1 mg/mL solution of EPS to 30 mL of $10^{-3}$ M (1 mM) of $HAuCl_4$ solution. The mixture was incubated at 35°C for 24 hrs in the dark (Sathiyanarayanan *et al*., 2014).

SNPs biosynthesis using POEPS was done by adding 20 ml of EPS solution to 20 ml of 10 mM aqueous solution of freshly prepared silver nitrate ($AgNO_3$) (Kanmani and Lim, 2013). The mixture was incubated at room temperature in the dark for 24-48 hrs.

*Biosynthesis of AuNPs and SNPs using POCFF and POFBE*

AuNPs biosynthesis using POCFF and POFBE was done by adding equal volumes of 1mM $HAuCl_4$ solution with CFF and POFBE, respectively. The mixture was incubated at 35°C in the dark (Nadaf and Kanase, 2016). Colour change from pale yellow to bluish purple indicated AuNPs formation.

SNPs biosynthesis using POCFF and POFBE was done by adding 50 mL of $AgNO_3$ solution (10 mM) to 10 mL of the POCFF and POFBE, respectively. The mixture was incubated at room temperature for 48 hrs in the dark (Zonooz and Salouti, 2011).

*Characterization of the biosynthesized AuNPs and SNPs*

The formation of AuNPs and SNPs was monitored by visual observation for a change in colour of the solutions in comparison to the control. Bio-oxidation and bio-reduction of gold and silver was measured periodically using UV–Vis spectrophotometer (a Lambda 25-Perkin Elmer, Waltham, MA, USA) with a resolution of 0.5 nm. The absorbance of the sample was read at the wavelengths of 200-800 nm.

Scanning Electron Microscopic was used to determine the size, shape and morphology of the biosynthesized nanoparticles. The aqueous solution of NPs synthesized were lyophilized and subjected to Scanning Electron Microscopy (SEM).

The functional groups present in the nanoparticles samples were determined using FTIR. The FTIR spectra of the dried KBr powdered nanoparticles samples were analysed using FTIR spectroscopy (Shimadzu) operated at resolution of 4 $cm^{-1}$. The spectra were recorded at a wave range of 500-4000 $cm^{-1}$.

*Antibacterial potential of the nanoparticles against some pathogens*

The antibacterial activity of the POEPSAuNPs, POCFFAuNPs and POFBEAuNPs POEPSSNPs, POCFFSNPs and POFBESNPs against some pathogens was determined using the agar well diffusion method (Shivashankar *et al*., 2013). The test pathogens used were: *K. pneumonia, Bacilus cereus, P. aeruginosa, Micrococcus* spp. *E. coli* and *S. aureus*). Suspension of 24-hour-old cultures of the test pathogens was done using saline. A lawn of the indicator strain was made by spreading the cell suspension over the surface of Mueller - Hinton agar plates with a sterile cotton swab. The plates were allowed to dry and wells were bored on the agar using a sterile cork borer of 7 mm diameter. Each well was filled with 20 µL of the biosynthesized AuNPs and SNPs. $HAuCl_4$ and $AgNO_3$ solution (1 mM), POEPS, POCFF and POFBE were used as negative controls. The seeded plates were incubated at 37°C for 24 hrs, the incubated plates were observed for zones of inhibition (ZOI) around the wells. Zone diameters (mm) greater than 1 mm were considered positive (Prabhu *et al*., 2014).

*Statistical analysis*

The statistical results are presented as the mean ± standard deviation (SD) at $P < 0.05$.

## Results

*Production of biomolecules from P. ostreatus*

Biomolecules (EPS and CFF and FBE) from *P. ostreatus* were used for mycosynthesis of gold

and silver nanoparticles. The nanoparticles were characterized and their antibacterial potential against some selected pathogens was investigated. Exopolysaccharide production by *P. ostreatus* (PO) is shown in Fig. 1. There was a significant difference (P≥ 0.05) in EPS production by PO on different days of incubation. EPS production by PO ranged from 300 - 3675.57 mg/L and the highest production was recorded on the 15th day.

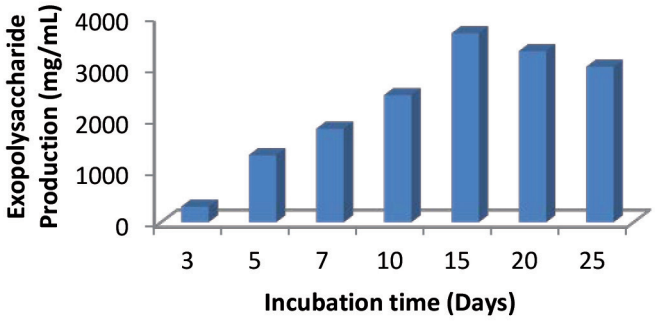


**Fig. 1.** Production of exopolysaccharides by *P. ostreatus*

*Biosynthesis and characterization of the nanoparticles*

Changes in colour were observed after the addition of the biomolecules to gold and silver nitrate solution. The visual observation of the biosynthesized POEPSAuNPs, POCFFAuNPs and POFBEAuNPs after incubation for 72 hrs is shown in Fig. 2a -2c. Colour changes from pale yellow to purple, cloudy colour and yellow colour to dark purple indicated the formation of POEPSAuNPs, POCFFAuNPs and POFBEAuNPs. The visual observation of the biosynthesized POEPSSNPs, POCFFSNPs and POFBESNPs is shown in Fig. 2d – 2f. Colour changes from pale yellow to dark brown indicated formation of POEPSSNPs while changes in colour from cloudy and pale yellow to dark brown indicated POCFFSNPs and POFBESNPs formation.

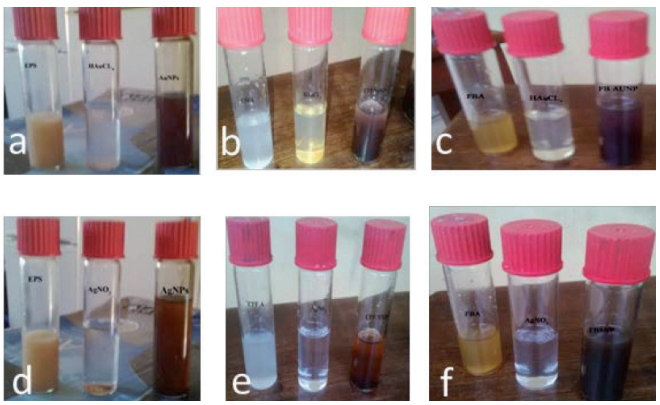


**Fig. 2**. Visual observation of (a) POEPSAuNPs, (b) POCFFAuNPs, (c) POFBEAuNPs (d) POEPSSNPs (e) POCFFSNPs and (f) POFBSNPs.

The absorption spectrum of the biosynthesized POEPSAuNPs, POCFFAuNPs and POFBEAuNPs after 72 hrs of incubation is shown in Figures 3a-c. The AuNPs gave absorbance peaks within the range of 200 - 800 nm after different hours of incubation. A strong SPR peak was observed at 500 nm and 600 nm.

The absorption spectra obtained from biosynthesized POEPSSNPs, POCFFSNPs and POFBESNPs at 72 hrs of incubation is shown in Figures 3 d - f. A sharp peak was recorded at 450 nm.

*Fourier Transform Infrared (FT-IR) analysis of the nanoparticles*

Figure 4a shows the spectra of biosynthesized AuNPs from the EPS of *P. ostreatus*. Eleven peaks were observed. The peak at 3429.17 $cm^{-1}$ gave a broad stretch of hydroxyl (O-H) while the peak at 2363.66 and 2335 $cm^{-1}$ corresponds to strong stretching carbon dioxide group (O=C=O). The peak at 1641.08 $cm^{-1}$ gave a medium conjugated alkene (C=C). A medium bending alkane from the methyl group of alkane (C-H) was seen at 1384.04 $cm^{-1}$. The peak at 1073.49 $cm^{-1}$ and 993.35 $cm^{-1}$ indicates a medium stretched amine group (C-N) and strong bending monosubstituted alkene (C=C), respectively. The peaks from 553.12 $cm^{-1}$ to 362.45 $cm^{-1}$ indicate the presence of alcohol (OH) bonds.

Figure 4b shows the spectra of AuNPs biosynthesized from the CFF of *P. ostreatus*. 8 peaks were observed. A broad stretching peak of carboxyl(O-H) was seen at 3418.68 cm-1 while the peak at 2096 $cm^{-1}$ corresponds to a strong stretching isothiocyonate group (N=C=S). The peak at 1633.72 $cm^{-1}$ indicates an aromatic ring stretch with a peak at 1446.4 $cm^{-1}$ and 1086.14 $cm^{-1}$ represents CO stretch from the COO- group. The peaks at 605.66 $cm^{-1}$, 467.3 $cm^{-1}$ and 390.51 $cm^{-1}$ indicate O-H alcohol group.

Figure 4c shows the FTIR spectra of AuNPs from the fruiting body of *P. ostreatus*. Sixteen (16) peaks were observed. The peak at 3428.85 indicates the hydroxyl stretching functional group while the peak at 2936.2 $cm^{-1}$ indicates weak CH stretch of methyl group. The peak at 2099.83 $cm^{-1}$ represents a strong stretch of isothiocyanate group of (N=C=S). The peak at 1641.84 $cm^{-1}$ shows the aromatic ring stretch and the peak at 1559.1 $cm^{-1}$ indicates a medium stretching cyclic alkene. The peaks at 1455.1 $cm^{-1}$ and 1402.42 $cm^{-1}$ could be assigned C=O stretch from the $COO^-$ group with the peak of 1306.5 $cm^{-1}$ indicating an aromatic amine? CN stretch. The peak at 1238.8 $cm^{-1}$ indicates phosphate group (P=O). The peak at 1084.15 $cm^{-1}$ cor-

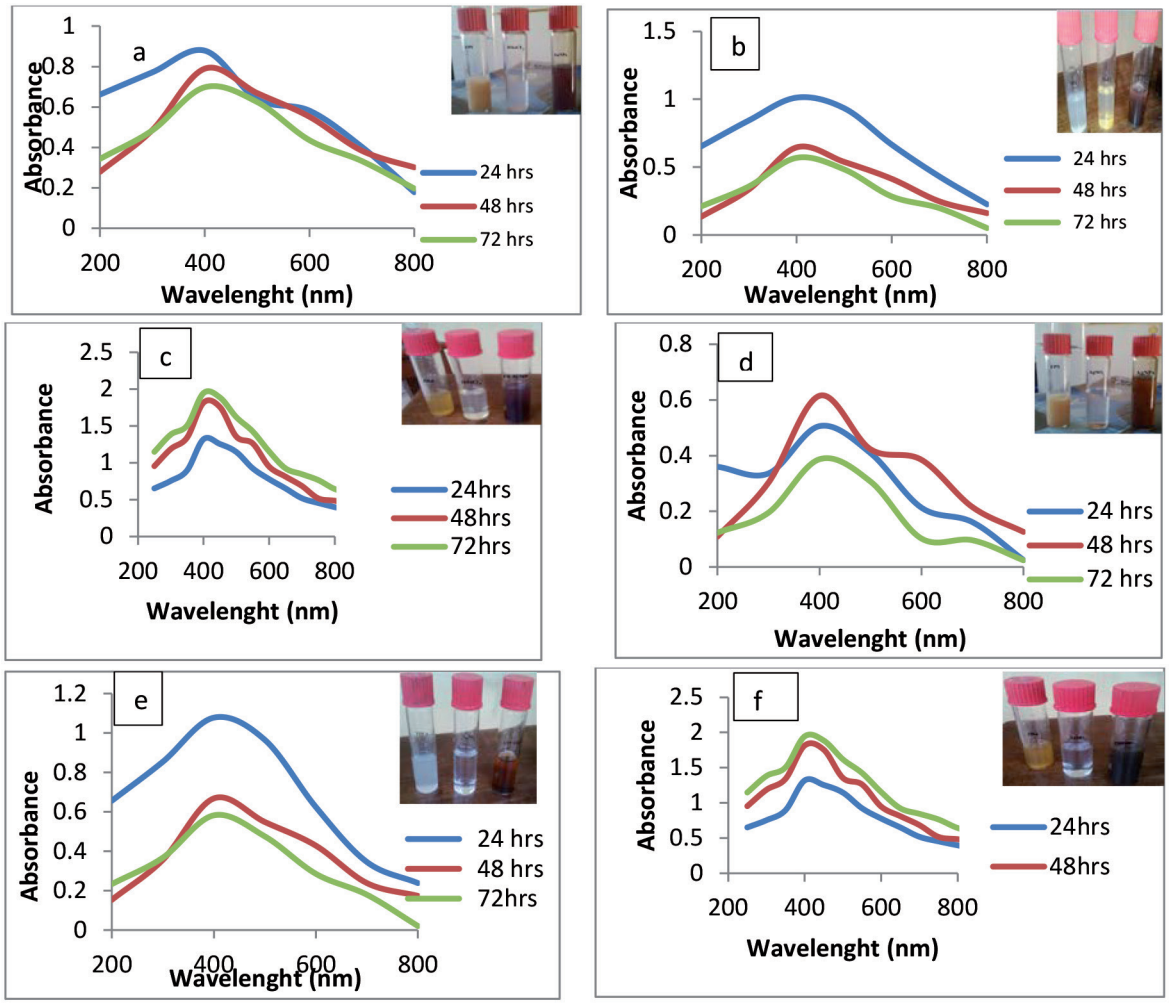


**Fig. 3.** UV-vis spectra of (a) POEPSAuNPs, (b) POCFFAuNPs, (c) POFBEAuNPs (d) POEPSSNPs (e) POCFFSNPs and (f) POFBSNPs.

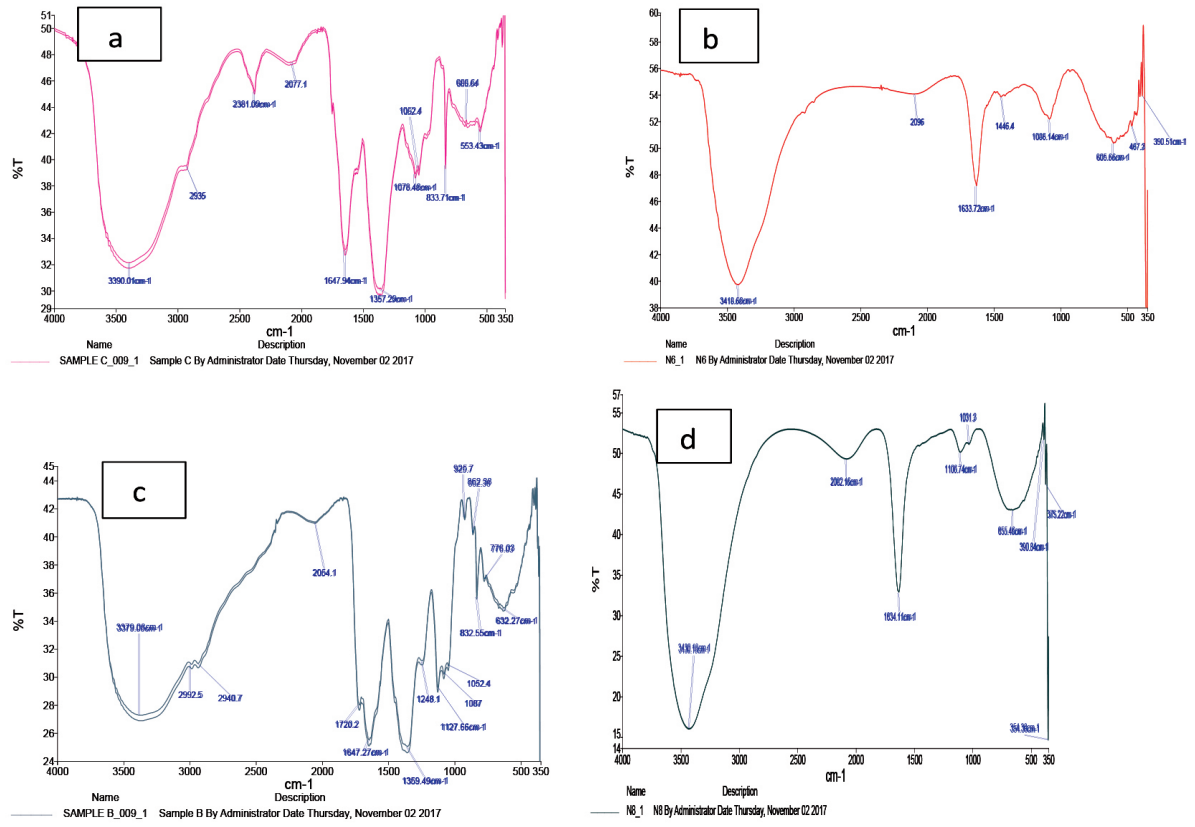


**Fig. 4.** FT-IR spectrum of (a) POEPSAuNPs (b) POCFFAuNPs, c) POFBEAuNPs (d) POEPSSNPs

responds to the C=O=C vibration in the glucopyranose ring. The peaks appearing from 999.7 $cm^{-1}$ are associated with the aromatic phosphate (P-O-C) stretch. The peaks appearing from 616.77cm $cm^{-1}$ to 363.59 $cm^{-1}$ represent the alcohol OH group.

Figure 4d shows the spectra of the biosynthesized SNPs from EPS of *P. ostreatus*. Nine (9) peaks were observed in which the peak at 3430.18 cm-1 indicates hydroxyl stretch of O-H group and the peak at 2082.16 $cm^{-1}$ indicates strong stretching isothiocyanate group (N=C=S). The peaks observed at 1106.74 and 1031.3 $cm^{-1}$ correspond to C-O-C vibration in the glucopyranose ring with the peaks at 655.46 $cm^{-1}$, 390.84 $cm^{-1}$ and 375.22 $cm^{-1}$ indicating an alcohol O-H group.

*Scanning Electron Microscopic analysis of AuNPs and SNPs from the biomolecules*

Figures 5 a-d show the micrograph of POEPSAuNPs, POCFFAuNPs, POEPSSNPs and POCFFSNPs. POEPSAuNPs was polymorphic in shape with 0.5 – 2.6 nm in size and 0.08 - 1.0 nm for POCFFAuNPs, POEPSSNPs and POCFFSNPs were aggregate with 2.2 – 3.0 nm and 0.2 – 2.8 nm in size, respectively.

*Antibacterial potentials of the biosynthesized nanoparticles and the biomolecules against some test pathogens*

Table 1a shows the antibacterial activity of the AuNPs and the biomolecules from *P. ostrateus* against the test pathogens. There was a significant difference in the antibacterial activity of the AuNPs against the test pathogens. The antibacterial activity of POEPSAuNPs, POCFFAuNPs and POFBEAuNPs against the test pathogens ranged from 21 – 28 mm, 8 - 22 mm and 9 – 29 mm. POEPSAuNPs, POCFFAuNPs and POFBEAuNPs exhibited the highest activity against *E. coli*, *Micrococcus* sp. and *P. aeruginosa,* respectively.

The antimicrobial activity of POEPS and POCFF ranged from 7 – 10 mm and 4 – 6 mm, with the highest activity recorded against *Micrococcus* sp. and *B. cereus*. POFBE did not have any observable antibacterial activity against the test pathogens. The antimicrobial activity of $HAuCl_4$ and ceftriaxone ranged from 1 – 7 mm and 16 – 26 mm, with the highest activity achieved against *B. cereus, K. pneumonia* and *E. coli*.

Table 1b shows the antibacterial activity of the SNPs and biomolecules from *P. ostrateus* against some selected test pathogens. A significant difference was observed in the antibacterial activity of the SNPs against the test pathogens. The antibacterial activity of POEPSSNPs, POCFFSNPs and POFBESNPs against the test pathogen ranged from 11 - 25 mm, 9 – 24 mm and 3 – 6 mm. POEPSSNPs, POCFFSNPs and POFBESNPs exhibited the highest activity against *B. cereus, S. aureus* and *E. coli*, respectively.

The antimicrobial activity of $AgNO_3$ and ceftriaxone against the test pathogens ranged from 4 – 9 mm and 16 – 26 mm. The highest activity was achieved against *P. aeruginosa, K. pneumonia* and *E. coli*.

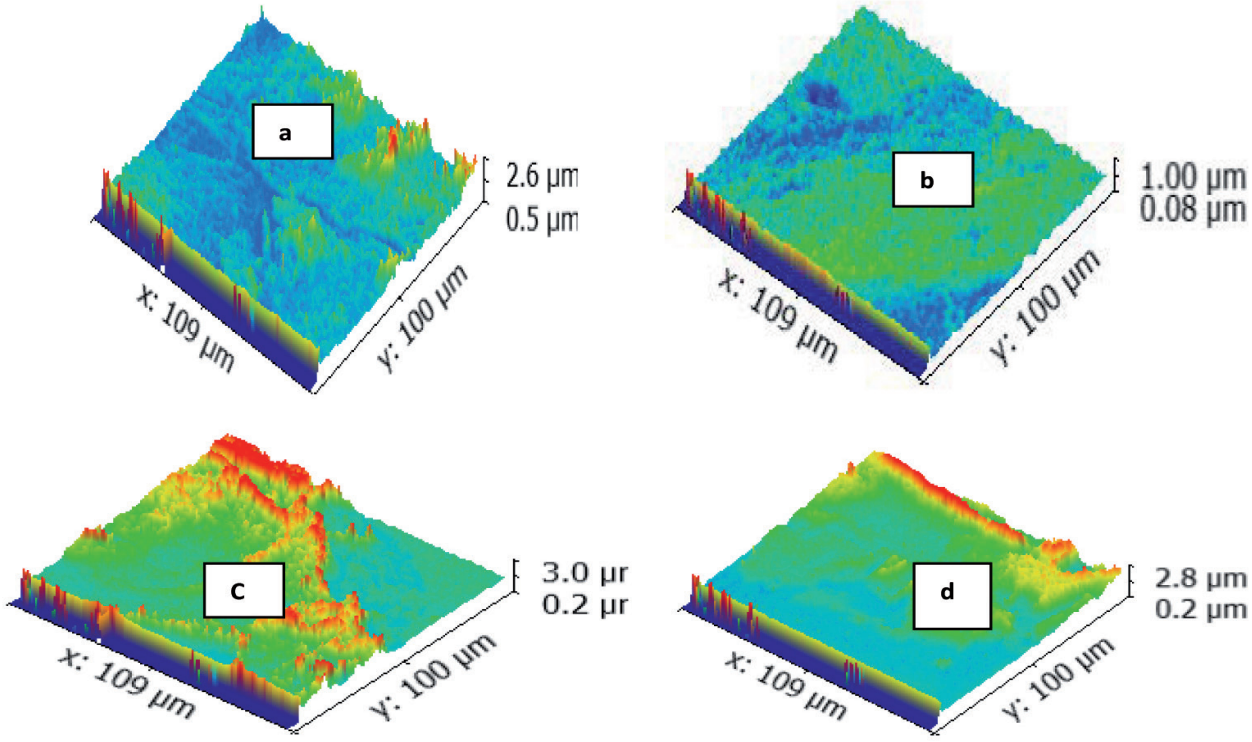


**Fig. 5**. SEM of micrograph of (a) POEPSAuNPs, (b) POCFFAuNPs, (c) POEPSSNPs and (d) POCFFSNPs

**Table 1a.** Antimicrobial activity of the biosynthesized AuNPs and the biomolecules against some pathogenic strains

| Zone of inhibition (mm) | | | | | | | | |
|---|---|---|---|---|---|---|---|---|
| **Test pathogen** | **POEPS AuNPs** | **POCF AuNPs** | **POFB AuNPs** | **POEPS** | **CFF** | **FB** | **$HAuCl_4$** | **CEFTR** |
| *K. pneumonia* | 26 | 8 | 13 | 9 | 4 | - | 2 | 26 |
| *B. cereus* | 27 | 18 | 16 | 7 | 6 | - | 7 | 16 |
| *P. aeruginosa* | 22 | 12 | 29 | 6 | 4 | - | 5 | 21 |
| *Micrococcus* sp. | 27 | 22 | 23 | 10 | 5 | - | 5 | 21 |
| *E. coli* | 28 | 12 | 28 | 7 | 5 | - | 0 | 26 |
| *S. aureus* | 21 | 11 | 9 | 6 | 4 | - | 1 | 22 |

**Table 1b.** Antimicrobial activity of the biosynthesized SNPs and the biomolecules against some pathogenic strains

| Zone of inhibition (mm) | | | | | | | | |
|---|---|---|---|---|---|---|---|---|
| **Test pathogen** | **POEPS SNPs** | **POCFF SNPs** | **POFBE SNPs** | **POEPS** | **CFF** | **FB** | **$AgNO_3$** | **CEFTR** |
| *K. pneumonia* | 14 | 19 | - | 9 | 4 | - | 6 | 26 |
| *Bacillus cereus* | 25 | 22 | - | 7 | 6 | - | 6 | 16 |
| *P. aeruginosa* | 11 | 9 | - | 6 | 4 | - | 9 | 21 |
| *Micrococcus* sp. | 19 | 23 | - | 10 | 5 | - | 8 | 21 |
| *E. coli* | 19 | 11 | 6 | 7 | 5 | - | 4 | 26 |
| *S. aureus* | 25 | 24 | 3 | 6 | 4 | - | 7 | 22 |

*Minimum Inhibitory Concentration (MIC) of the nanoparticles*

The minimum inhibitory concentration (MIC) of the biosynthesized nanoparticules is shown in Table 2. The MIC of 200 µg/mL was observed for all the test pathogens when the biosynthesized POEPSAuNPs and POCFFAuNPs were used as antimicrobial agents. There was variation in the MIC of the biosynthesized SNPs against the test pathogens. POEPSSNPs hada MIC of 6.25 µg/ml against *E. coli,* 50 µg/ml against *P. aeruginosa, B. cereus, S. aureus* and *Micrococcus* sp. and 100 µg/mL against *K. pneumoniae.*

POCFFSNPs had a MIC of 12.5 µg/mL against *E. coli* while the MIC of 50 µg/mL as recorded against *P. aeruginosa, B. cereus S. aureus* and *Micrococcus* sp. Ceftriaxone had an MIC of 5 µg/mL against *P. aeruginosa, B. cereus, E. coli, S. aureus* and *Micrococcus* sp. An MIC of 10 µg/mL was observed against *K. pneumonia*.

The EPS and CFS from *P. ostreatus* were used for the biosynthesis of AuNPs and SNPs. The biosynthesized nanoparticles were characterized and their antibacterial activities against the test pathogens were evaluated.

**Table 2.** Minimum Inhibitory Concentration of biosynthesized nanoparticles from *P. ostreatus*

| **Nanoparticle samples** | **Minimum Inhibitory Concentration (µg/ml)** | | | | | |
|---|---|---|---|---|---|---|
| | *P. aeruginosa* | *B. cereus* | *K. pneumonia* | *Microoccus* sp. | *E. coli* | *S. aureus* |
| POEPSAuNPs | 200 | 200 | 200 | 200 | 200 | 200 |
| POCFF AuNPS | 200 | 200 | 200 | 200 | 200 | 200 |
| POFB EAuNPS | 100 | 200 | 200 | 200 | 200 | 200 |
| POEPSSNPs | 50 | 50 | 100 | 50 | 6.25 | 50 |
| POCFFSNPs | 50 | 50 | 100 | 50 | 12.5 | 50 |
| POFBESNPs | 25 | 25 | 50 | 50 | 12.5 | 50 |
| Ceftriaxone | 5 | 5 | 10 | 5 | 5 | 5 |

## Discussion

*EPS-production by P. ostreatus*

*P. ostreatus* produced a reasonable quantity of exopolysaccharides. Reduction in EPS- production after 15th day of incubation may be due to the exhaustion of the available nutrient in the production medium. This was also recorded by Olfat and Sadik (2014), who worked on the production of EPS and bioactive metabolites in a submerged culture of *P. ostreatus*. A different report was obtained in the work of Adebayo-Tayo *et al.* (2011), where there were fluctuations in EPS production by *P. ostreatus* during optimization of the growth conditions, which was ascribed to the different media composition.

*Biosynthesis of AuNPs and SNPs by P. ostreatus biomolecules*

Biosynthesis of silver nanoparticles using EPS from *Pleurotus* sp. was achieved via the bio-reduction method. Other methods of biosynthesis have also been reported. Ravishankar *et al*. (2011) used photo-irradiation method to biosynthesize SNPs from an aqueous extract of *Pleurotus florida*; Sujatha *et al*. (2013) also synthesized SNPs from edible mushroom extracts, such as *Agaricus bisporus, Calocybe indica, P. florida* and *P. platypus*. CFF was also used in the biosynthesis of NPs. Abdelmageed *et al*. (2016) synthesized NPs using an extracellular supernatant of *Penicillium politans*; Soheyla *et al.* (2013) reported a green process for production of silver (Ag) nanoparticles using *Penicillium chrysogenum*; Kumar and Ghosh (2016) biosynthesized silver nanoparticles from silver nitrate using *Bacillus* sp. (*Brevibacillus borstelensis* MTCC10642).

Biosynthesis of AuNPs from EPS produced by *Pleurotus* sp. has not been reported though CFF has been used in the biosynthesis of nanoparticles. Michael *et al*. (2015) reported the biosynthesis of AuNPs from fungi and their protein extracts.

*Characterization of the biosynthesized nanoparticles*

The appearance of a pale yellow to purple colour indicated the oxidation of the chloroauric acid ions by the fungal biomolecules, which resulted in the formation of gold nanoparticles. Changes in colour were due to the excitation of surface plasmon vibrations, which is a characteristic feature of synthesized nanoparticles (Song *et al.*, 2009). This was in agreement with other studies. Gitanjali and Ashok (2014) reported the biosynthesis of AuNPs from observing the gradual change in colour thus concluding that the colour of nanaoparticles from *Herbarium tetramera* periodically change from different shades to purple, which indicated preliminary test in the formation of AuNPs.

The yellowish brown colour formation by SNPs has been confirmed by many researchers (Hany et al., 2014). The metal salt bio-reduction ability of the fungal filtrate for nanoparticles biosynthesis with an observable colour change has been attributed to the surface plasmon resonance of deposited SNPs (Mulvaney, 1996). Balakumaran *et al.* (2016) also reported that the change of colour to brown was a result of SPR vibration excitation. Characteristic changes in colour may be attributed to the alteration in surface plasmon resonance (SPR) when positive ions (Ag+) are transformed into nano-forms (Mital, 2013).

Characterization of metal ions exposed to the biomolecules of *P. ostreatus* by UV-Vis spectrophotometer confirmed the reduction of metal ions to metal nanoparticles. Metallic nanoparticles exhibit an intense UV absorption band due to SPR effect. Mie's theory proposed SPR arose from the interaction of small metallic particles with an external electromagnetic field induced by light, resulting in a coherent oscillation of the conductor free electrons on the surface (Mie, 1908). These confirm the formation of NPs. The SPR peak obtained for the AuNPs synthesized using the different samples in this work was observed at 500 nm. Typically, AuNPs have a maximum wavelength in the visible range of 500 nm - 600 nm (Oba *et al*., 2009; Barabadi *et al*., 2014; Shivaji *et al.*, 2014). The SNPs formed from other biomolecules was also confirmed using the UV spectrophotometer and are seen in the range of 400 -500 nm. This is referred to as the SPR of the SNPs with strong peaks between 400 nm – 450 nm. This result agrees with the report of Gannimani *et al*. (2014), who biosynthesized SNP from aqueous seed extract of *Protorhus longifolia*. Hany *et al*. (2014) produced SNP from the CFF of different fungi with peaks, which was due to the surface resonance and vibration of electrons. These peaks are known as SPR (Mansoori *et al*., 2007). Raza *et al*. (2016) reported that the presence of a single SPR peak indicates that the particles were spherical with a wide range of size distribution. Formation of an SPR peak in the range of 410–450 nm has been attributed to the biosynthesis of AgNP. This occurs as a result of alteration in the surface plasmon resonance (SPR) when positive ions (Ag+) are transformed into nano-forms.

The active compounds in the biomolecules

involved in the reduction of metal ions for metal nanoparticle formation were investigated using FTIR. It confirmed that biomolecules such as EPS, CFF and FBE were responsible for capping and efficient stabilization of the metal nanoparticles synthesized. This makes fungi extremely good candidates in the synthesis of metal nanoparticles that are safe and eco-friendly. The spectrum of the biomolecules extract exhibited intense and distinct absorption bands at 1720 and 3317 $cm^{-1}$, which correspond to the amide, carboxyl and hydroxyl bands. Formation of stronger bonds between the biomolecules (EPS, CFF and FBE) and the metal ions may be as a result of the presence of the functional groups (carboxylic, hydroxyl and amide groups) in the biomolecules. The presence of the amide linkage suggests that there are some proteins in the reaction mixture which may be responsible for nanoparticles formation and may play an important role in the stabilization of the formed nanoparticle. The bands of aromatic and aliphatic amines, respectively, are also observed, which is similar to the earlier reports of Ashajyothi *et al*. (2014) on biosynthesis and characterization of NPs from gram-negative bacteria biomass. These bands are close to those reported for natural phytochemicals in the *Agaricus biporus* extract. Thus, nano capping of the particles from EPS, CFF and FBE of *P. ostreatus* are responsible for reduction and subsequent stabilization of Au-NPs.

The SEM micrograph of the gold and silver nanoparticles shows polymorphic and aggregated particle shapes due to the capping agent. This result agrees with the work of Adebayo-Tayo *et al*. (2017), who reported on the bacterial synthesis of nanoparticles from the supernatant of lactic acid bacteria.

The antimicrobial potential of nanoparticles was also examined in this report. The activity of gold chloride (positive control) on bacteria isolate was minimal compared to the nanoparticles. Gold ions as well as AuNPs are known to have strong antimicrobial activities. The antimicrobial ability of Au nanoparticles might be due to their small size (which is 250 times smaller than a bacterium), which makes their adhesion to the cell wall of microorganisms easier, thus leading to destruction and cell death (Chwalibog *et al*., 2010). Metal nanoparticles are also harmful to bacteria due to their ability to disrupt the membrane protein and sulphur components. They bind closely to the surface of microorganisms causing visible damage to the cells, thus demonstrating good self-assembling ability. Gold nanoparticles possess well-developed surface chemistry, chemical stability and appropriate smaller size, which facilitate their interaction with microorganisms (Nirmala and Pandian, 2007). Also, the particles interact with the building elements of the outer membrane and might cause structural changes, degradation and finally cell death. The test pathogens were susceptible to the NPs biosynthesized using biomolecules of *P. ostreatus.*

## Conclusion

EPS, CFS and FBE of *P. ostreatus* were able to bio-reduce and bio-oxidize silver and gold for the biosynthesis of SNPs and AuNPs, respectively. The AuNPs had a broad spectrum of activity against the test pathogenic strains compared to the SNPs. These nano-biocomposites can be used in the formulation of novel antibacterial agents and can be applied in biomedical fields.

## References


Abdelmageed, M., A. Maysa, M. Elsayed, M. Mohamed (2016). Silver nanoparticles (AgNPs) were successfully synthesized using an extracellular supernatant of *Penicillium politans*. *Inter. J. Pharm. Technol. Res*. **9**: 433-444.

Adebayo-Tayo, B. C., S. G. Jonathan, O. O. Popoola, R. C. Egbomuche (2011). Optimization of growth conditions for mycelia yield and exopolysaccharide production by *Pleurotus ostreatus* cultivated in Nigeria. *Afr. J. Microbiol. Res.* **5**:130-2138.

Adebayo-Tayo, B. C., A. O. Popoola., O. M. Ajunwa (2017). Bacterial synthesis of silver nanoparticles by culture free supernatant of lactic acid bacteria isolated from fermented food samples. *Biotechnol. J. Int.* **19**: 1-13.

Aitken, R. J., M. Q. Chaudhry, A. B. A. Boxall, M, Hull (2006). Manufacture and use of nanomaterial: current status in the UK and global trends. *Occupational Med.* **56**: 300–306.

Akinoglu, E. M., A. J. Morfa, M. Giersig (2014). Nanosphere lithography - exploiting self-assembly on the nanoscale for sophisticated nanostructure fabrication. *Turk. J. Phys.* **38**: 563–572.

Amar, K., G. Ashok (2016). Biosynthesis of silver nanoparticules with bacteria isolated from gangetic-alluvial soil. *Int. J. Biotechnol. Biochem*. **12**: 95-102.

Ashajyothi, C., P. Gunasekaran (2014). Green synthesis of silver nanoparticles using the mushroom fungus *Schizophyllum commune* and its biomedical applications. *Biotechnol. Bioprocess Eng*. **19**: 1083-1090.

BalaKumaran, M. D., R. Ramachandran, S. Jagadeeswari, T. K. Puthupalayam (2016). *In vitro* biological properties and characterization of nanosilver coated cotton fabrics – an application for antimicrobial textile finishing. *Int. Biodeter. Biodegrad*. **107**: 48-55.

Balashanmugam, P., S. Santhosh, H. Giyaullah, M. D. Balakumaran, P. T. Kalaichelvan (2013). Mycosynthesis, characterization and antibacterial activity of silver nanoparticles from *Microporus xanthopus*: a macro-mushroom. *Int. J. Innov. Res. Sci. Eng. Technol.* **2**: 1-9.

Barabadi, H., S. Honary, P. Ebrahimi, M. Ali, A. Alizadeh, F. Naghibi (2014). Microbial mediated preparation, charac-

terization and optimization of gold nanoparticles. *Braz. J. Microbiol*. **45**: 1493-1501.

Castro-Longoria, E., A. R. Vilchis-Nestor, M. Avalos-Borja (2011). Biosynthesis of silver, gold and bimetallic nanoparticles using the filamentous fungus *Neurospora crassa*. *Colloids Surf. B. Biointerfaces* **83**: 42–48.

Chwalibog, A., E. Sawosz, A. Hotowy, J. Szeliga, S. Mitura, K. Mitura, M. Grodzik, P. Orlowski, A. Sokolowska (2010). Visualization of interaction between inorganic nanoparticles and bacteria or fungi. *Int. J. Nanomed*. **5**: 1085–1094.

Costa, P., A. Amaro, A. Botelho (2010). Gold nano probe assay for the identification of mycobacteria of the *Mycobacterium tuberculosis* complex. *Clin. Microbiol. Infect*. **16**: 1464–1469.

Cui, J., K. K. Goh, R. Archer, H. Singh (2007). Characterization and bioactivity of protein- bound polysaccharides from submerged-culture fermentation of *Coriolus versicolor* Wr-74 and ATCC-20545 strains. *J. Ind. Microbiol. Biotechnol*. **34**: 393–402.

Demir, E., N. Kaya, B. Kaya (2014). Genotoxic effects of zinc oxide and titanium dioxide nanoparticles on root meristem cells of *Allium cepa* by comet assay. *Turk. J. Biol.* **38**: 31–39.

Dubois, M., K. A. Gilles, J. K. Hamilton, P. A. Rebers, F. Smith, (1956). Colorimetric method for determination of sugars and related substances. *Anal. Chem.* **28**: 350-356.

Fayaz, A. M., K. Balaji, M. Girilal (2009). Biogenic synthesis of silver nanoparticles and their synergistic effect with antibiotics: a study against gram-positive and gram-negative bacteria. *Nanomed*. **6**: 103–109.

Felek, W., F. Mekibib, B. Admassu (2015). Optimization of explants surface sterilization condition for field grown peach (*Prunus persica* L. Batsch. Cv. Garnem) intended for in vitro culture. *Afr. J. Biotechnol.* **14**: 657-660.

Gannimani, R., A. Perumal, S. B. Krishna, K. Muthusamy, A. Ishra, P. Govender (2014). Synthesis and antibacterial activity of silver and gold nanoparticles produced using aqueous seed extract of *Protorhus longifolia* as a reducing agent. *Digest J. Nanomat. Biostruc.* **9:** 1669-1679.

Ghosh, P., G. Han, K. C. DeMrinmoy, R. Kyu, M. Vincent (2008). Gold nanoparticles in delivery applications. *Adv. Drug. Del. Rev*. **60**: 1307–1315.

Gitanjali, B. S., M. C. Ashok (2014). Extracellular biological synthesis, characterization and stability of gold nanoparticles using the fungus *Helminthosporium tetramera. IJPAB* **2**: 281-285.

Hany, M., H. E. Magdi, M. Mourad, A. El-Aziz (2014). Biosynthesis of silver nanoparticles using fungi and biologicalevaluation of mycosynthesized silver nanoparticles. *Egypt. J. Exp. Biol.* **10**: 1-12.

Jonathan, S. G., L. T. Kigigha, E. Ohimain (2008). Evaluation of the inhibitory potentials of edible higher Nigerian fungi against pathogenic microorganisms. *Afr. J. Biomed. Res.* **11**: 195-200.

Kanmani, P., S. T. Lim (2013). Synthesis and structural characterization of silver nanoparticles using bacterial exopolysaccharide and its antimicrobial activity against food and multidrug resistant pathogens. *Process Biochem.* **48**: 1099-1106.

Kato, H. (2011). *In vitro* assays: tracking nanoparticles inside cells. *Nat. Nanotechnol.* 6: 139–140.

Kim, Y. C., N. C. Park, J. S. Shin, S. R. Lee, Y. J. Lee, D. J. Moon (2003). Partial oxidation of ethylene to ethylene oxide over nanosized Ag/α-Al2O3 catalysts. *Catalyst Today,* **87**: 153–162.

Krishna, A. G., R. V. S. N. Ravikumar, T. V. Kumar, S. D. Ephraim, B. Ranjith, M. Pranoy, S. Dola (2016). Investigation and comparison of optical and Raman bands of mechanically synthesized $MoO_3$ nano powders. *Mat. Today Proc.* **3**: 54-63.

Mansoori, G. A., T. F. George, G. Zhang, G., L. Assoufid (2007). Molecular Building Blocks for Nanotechnology, Springer, New York, pp. 418.

Marini, M., N. De Niederhausern, R. Iseppi, M. Bondi, C. Sabia, M. Toselli (2007). Antibacterial activity of plastics coated with silver-doped organic-inorganic hybrid coatings prepared by sol–gel processes. *Biomacromolecules* **8**: 1246-1254.

Mata, M. T., F. Baquero, J. C. Perez-Diaz (2000). A multidrug efflux transporter in *Listeria monocytogenes. FEMS Microbiol. Lett.* **187**: 185-188.

Micheal, K., R. Meghana, M. Enrico (2015). Fungal biosynthesis of gold nanoparticles: mechanism and scale up. *Microb. Biotechnol.* **8**: 904–917.

Mittal, A. K., Y. Chisti, U. C. Banerjee (2013). Synthesis of metallic nanoparticles using plant extracts. *Biotechnol. Adv.* **31:** 346–356.

Mulvaney, P. (1996). Surface plasmon spectroscopy of nanosized metal particles. *Langmuir* **12**: 42-123.

Nadaf, N. Y., S. S. Kanase (2016). Biosynthesis of gold nanoparticles by *Bacillus marisflavi* and its potential in catalytic dye degradation. *Arab. J. Chem.* **12**: 4806-4814.

Nirmala, G. A., K. Pandian, C. A. Surfa (2007). Antibacterial efficacy of aminoglycosidic antibiotics protected gold nanoparticles, a brief study. *Colloid. Surf. A: Physicochem. Eng. Asp.* **297**: 63-70.

Oba, K., S. Teramukai, M. Kobayashi, T. Matsui, Y. Kodera, J. Sakamoto (2007). Efficacy of adjuvant immunochemotherapy with polysaccharide K for patients with curative resections of gastric cancer. *Cancer Immunol. Immunother.* **56**: 905-911.

Olfat, S. B., M. W. Sadik (2014). Mycelial growth and bioactive substance production of *Pleurotus ostreatus* in submerged culture. *Intern. J. Cur. Microbiol. Appl. Sci*. **3**: 1073-1085.

Phanjom, P., G. Ahmed (2015). Biosynthesis of silver nanoparticles by *Aspergillus oryzae* (MTCC No. 1846) and its characterizations. *Nanosci. Nanotechnol*. **5**: 14-21.

Pissuwan, D., C. Cortie, S. Valenzuela, M. Cortie (2010). Functionalised gold nanoparticles for controlling pathogenic bacteria. *Trend. Biotechnol.* **28:** 207-213.

Pissuwan, D., T. Nidome, M. B. Cortie (2011). The forthcoming applications of gold nanoparticles in drug and gene delivery systems. *J. Control Rel*ease **149**: 65-71.

Prabhu, S. S., R. K. Mohan, P. Sanhita, R. Ravindran (2014). Production of bacteriocin and biosynthesis of silver nanoparticles by lactic acid bacteria isolated from yoghurt and its antibacterial activity. *Scrutiny Int. Res. J. Microbiol. Biotechnol.* **1**: 7-14.

Rai, M., A. Yadav, A. Gade (2009). Silver nanoparticles as a new generation of antimicrobials. *Biotechnol. Adv.* **27**: 76-83.

Ravishnkar, B., D. Raghunandan, V. G. Sharanabasava, H.

Do Shung, A. Venkataraman (2011). Photo-irradiated biosynthesis of silver nanoparticles using edible mushroom *Pleurotus florida* and their antibacterial activity studies. *Bioinorg. Chem. Appl.* **2011**: Article ID 650979.

Raza, M. A., Z. Kanwal, A. Rauf, (2016). Size- and shape-dependent antibacterial studies of silver nanoparticles synthesized by wet chemical routes. *Nanomaterials* **6**: 74.

Rezaei-Zarchi, S., S. Imani, Z. Mohammad, M. Saadati, (2012). Study of bactericidal properties of carbohydrate stabilized platinum oxide nanoparticles. *Inter. Nanotechnol. Lett.* **2**: 40–45.

Saha, K., S. S. Agasti, C. Kim, X. Li, V. M. Rotello (2012). Gold nanoparticles in chemical and biological sensing. *Chem. Rev.* **112**: 2739-2779.

Sathiyanarayanan, G., V. Vignesh, G. Saibaba, A. Vinothkanna, K. Dineshkumar, M. B. Viswanathan, J. Selvin (2014). Synthesis of carbohydrate polymer encrusted gold nanoparticles using bacterial exopolysaccharide: A novel and greener approach. *RSC Advan.* **4**: 22817-22827.

Shivaji, S. W., M. D. Arvind, S. Zygmont (2014). Biosynthesis, optimization, purification and characterization of gold nanoparticles. *Afr. J. Microbiol. Res.* **8**:138-146.

Shivashankar, M., B. Premkumari, N. Chandan (2013). Biosynthesis, partial characterization and antimicrobial activities of silver nanoparticles from *Pleurotus* species. *Int. J. Integ. Sci. Innov. Technol.* **2**: 13-23.

Soheyla, H., B. Hamed, G. F. Eshrat, N. Farzaneh (2013). Green synthesis of silver nanoparticles induced by the fungus *Penicillium citrinum*. *Trop. J. Pharm. Res.* **12**: 7-11.

Song, J. Y., B. S. Kim (2009). Biological synthesis of bimetallic Au/Ag nanoparticles using Persimmon (Diospyros kaki) leaf extract. *Korean J. Chem. Eng.* **25**: 808–811.

Sujatha, S., S. Tamilselvi, K. Subha, A. Panneerselvam (2013). Studies on biosynthesis of silver nanoparticles using mushroom and its antibacterial activities. *Intern. J. Cur. Microbiol. Appl. Sci.* **12**: 433-444.

Zonooz, N. F., M. Salouti (2011). Extracellular biosynthesis of silver nanoparticles using cell filtrate of *Streptomyces* sp. ERI-3. *Iran J. Sci. Technol*. **1**: 1631-1635.